



7th Trondheim CCS Conference, TCCS-7, June 5-6 2013, Trondheim, Norway

## CaZrO<sub>3</sub> and SrZrO<sub>3</sub>-based CuO Oxygen Carriers for Chemical-Looping with Oxygen Uncoupling (CLOU)

Mehdi Arjmand<sup>a,\*</sup>, Abdul-Majeed Azad<sup>b,c</sup>, Henrik Leion<sup>a</sup>, Magnus Rydén<sup>c</sup>,  
Tobias Mattisson<sup>c</sup>

<sup>a</sup>Department of Chemical and Biological Engineering, Division of Environmental Inorganic Chemistry, Chalmers University of Technology, SE-412 96 Göteborg, Sweden

<sup>b</sup>Department of Chemical Engineering, The University of Toledo, Toledo, OH 43606-3390 USA

<sup>c</sup>Department of Energy and Environment, Division of Energy Technology, Chalmers University of Technology, SE-412 96 Göteborg, Sweden

### Abstract

The chemical-looping combustion (CLC) and chemical-looping with oxygen uncoupling (CLOU) processes are novel solutions for efficient combustion with inherent separation of carbon dioxide. In this work, oxygen carriers based on CuO supported by zirconates of SrZrO<sub>3</sub> and CaZrO<sub>3</sub> are investigated. The oxygen carriers were produced by mechanical homogenization of primary solids in a rotary evaporator followed by extrusion, drying and calcination at 950 and 1030°C for 6 h. Their chemical-looping performance was evaluated in a laboratory-scale fluidized-bed reactor at 900 and 925°C under cyclic oxidizing, inert (N<sub>2</sub>) and reducing (CH<sub>4</sub>) conditions. All oxygen carriers exhibited rapid release of oxygen in the inert environment (CLOU) with high conversion of methane. The carrier calcined at 1030°C with SrZrO<sub>3</sub> as support showed no agglomeration or deactivation and exhibited the highest reactivity. Thus, the use of this oxygen carrier could be of interest for the CLOU process.

© 2013 Published by Elsevier Ltd. This is an open access article under the CC BY-NC-ND license (<http://creativecommons.org/licenses/by-nc-nd/3.0/>).

Selection and peer-review under responsibility of SINTEF Energi AS

**Keywords:** CO<sub>2</sub>-capture; chemical-looping combustion (CLC); chemical-looping with oxygen uncoupling (CLOU); oxygen carrier; copper oxide; zirconate

### 1. Introduction

As suggested by the intergovernmental panel on climate control (IPCC), a 50-85% reduction in total CO<sub>2</sub> emission by 2050 is necessary to limit the anticipated global temperature rise to 2°C [1]. A number

\* Corresponding author. Tel.: +46-31-772-2822; Fax: +46-31-772-2853.  
E-mail address: [arjmand@chalmers.se](mailto:arjmand@chalmers.se).

of alternative technologies have been proposed to mitigate the rising levels of carbon dioxide in the atmosphere. Among these, carbon capture and storage (CCS) is considered promising.

Chemical-looping combustion (CLC) can give an essentially pure CO<sub>2</sub> stream from hydrocarbon combustion without any direct gas separation. In a CLC system, two reactors, a fuel reactor and an air reactor, are interconnected with an oxygen carrier circulating between these reactors [2-4]. When fuel and air are introduced into the reactors, the following overall reactions occur, i.e. reaction (1) in the fuel reactor, and reaction (2) in the air reactor,



Here,  $Me_xO_y$  and  $Me_xO_{y-1}$  are the oxidized and reduced forms of an oxygen carrier.  $C_nH_{2m}$  is the fuel, which could be gas, liquid or solid. A schematic description of the process is shown in Figure 1. In case of complete conversion of the fuel, the exhaust stream from the fuel reactor consists of only CO<sub>2</sub> and H<sub>2</sub>O, from which pure CO<sub>2</sub> could be obtained after condensation of water. The reduced oxygen carrier ( $Me_xO_{y-1}$ ) is then transferred to the air reactor where it is re-oxidized by air making it ready for the next cycle. Thus in CLC, N<sub>2</sub> and CO<sub>2</sub> gases are never mixed. The oxidation reaction is always exothermic while the reduction reaction can be exothermic or endothermic depending on the fuel and the oxygen carrier [5]. However, the sum of the heat from reactions (1) and (2) is the same as for conventional combustion. Thus the CLC process does not entail any direct energy penalty for CO<sub>2</sub> separation. CLC has been successfully demonstrated in a number of units of sizes up to 120 kW [6]. Overviews of current achievements in CLC are given by Lyngfelt [6, 7], Hossain and de Lasa [8] and Adanez et al. [9]

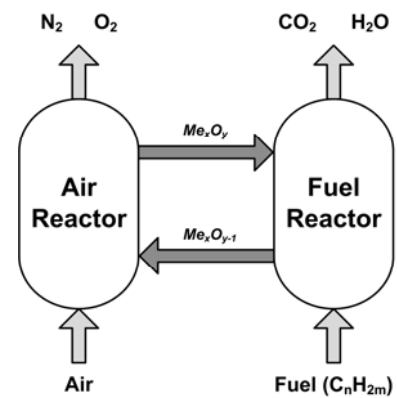
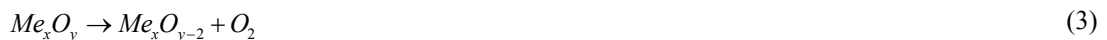


Fig. 1 Schematic of the chemical-looping combustion (CLC) process

In the case of solid fuels, the char remaining after devolatilization is gasified in the presence of steam, producing CO and H<sub>2</sub>, which then react with the oxygen carrier. An alternative to CLC for solid fuels using gasification of the char, is chemical-looping with oxygen uncoupling (CLOU) [10], in which the char reacts directly with gaseous oxygen released from the oxygen carrier. In comparison to CLC where the reduction of oxygen carrier and oxidation of the gaseous fuel generally occurs in a single step, an additional step is needed in CLOU for the release of gaseous oxygen from the carrier prior to conversion of the fuel according to



This is followed by the normal combustion of the fuel via



The reduced oxygen carrier is transferred to the air reactor for re-oxidation. The overall heat of reaction for the CLOU process is the same as CLC and only the mechanism by which oxygen is accessed by the fuel differs. However, when using solid fuels like coal, the CLOU process avoids the slow

gasification of the solid fuel needed to produce synthesis gas as a prerequisite for the reaction with the oxygen carrier [10]. The oxygen carrier in CLOU must be able to both react with  $O_2$  and release  $O_2$  at temperatures suitable for the process, i.e. 800 to 1200°C.

The most commonly proposed approach to realize CLC is to use inter-connected fluidized-bed reactors in a similar fashion as in a circulating fluidized-bed boiler (CFB) [2], the difference being that CLC will require an active oxygen carrier rather than inert sand as bed material. Conventional CFB boilers often operate at an air to fuel ratio of about 1.2, which in the case of CLC corresponds to an outlet oxygen concentration close to 5% from the air reactor. To be noted is that this concentration is somewhat higher than in normal combustion since the flue gas from the air reactor does not contain  $CO_2$ . Therefore, oxide systems with an equilibrium oxygen partial pressure lower than 5% at temperatures typical of the air reactor are desirable. Otherwise, higher air ratio will be required compared to conventional combustion, which would result in a higher heat loss due to larger flue gas stream. Moreover, the oxygen carrier should also be able to release a sufficiently large amount of oxygen in the fuel reactor, at a sufficiently high rate.

An important aspect in the development of CLC and CLOU processes is the selection of oxygen carrier materials with adequate reactivity. Oxides of transition metals (Mn, Fe, Co, Ni and Cu), their mixtures, and a number of natural minerals (ores), industrial wastes and by-products have been investigated as oxygen carriers in CLC and CLOU [6-9]. High reactivity during oxidation and reduction over large number of cycles and the ability to fully convert the fuel are sought-after characteristics. In addition, thermal and mechanical stability, proper fluidization characteristics and resistance to attrition and agglomeration are also important. One way of achieving these properties is to mix the active phase (carrier oxide) with an inert support such as  $TiO_2$ ,  $SiO_2$ ,  $ZrO_2$ ,  $Al_2O_3$  or  $MgAl_2O_4$  and/or heat-treat the oxygen carriers [8].

Copper-oxide materials have received a great deal of attention as efficient oxygen carriers, owing to high reactivity, high oxygen transport capacity and absence of thermodynamic limitation for complete combustion of the fuel [6-9]. Among various supports for CuO oxygen carriers,  $Al_2O_3$  has received considerable attention [11-22]. However, when using  $Al_2O_3$  as support, a difficulty arises due to the facile interaction between CuO and  $Al_2O_3$  either during synthesis or during operation, resulting in partial loss of CuO and CLOU behaviour due to formation of copper (II) aluminate ( $CuAl_2O_4$ ) and copper (I) aluminate ( $CuAlO_2$ ; delafossite) [11-22]. Since the copper-aluminate phases are highly reducible, the interaction between the support and the active phase does not necessarily cause a problem with respect to CLC application. For CLOU however, this interaction should be avoided in order to preserve CuO as the active phase, for instance by using other supports such as  $TiO_2$ ,  $ZrO_2$ ,  $SiO_2$  or  $MgAl_2O_4$ .

Most of the studies using Cu-based oxygen carriers have been carried out at low temperatures (~800°C) where CLOU effect is small, i.e. application for CLC [6-9]. However at higher temperatures (~950°C), an increase of carbon conversion rate in the vicinity of CuO particles had been reported which was associated with the direct oxidation of char [23]. It is now well established that CuO decomposes to  $Cu_2O$  when the actual concentration of oxygen is lower than the equilibrium concentration [10]. As a result, oxygen is released thereby allowing CLOU to take effect. For temperatures of 900 and 925°C, this occurs at oxygen concentrations below 1.5 and 2.7%, respectively [10]. Thus, from a CLOU point of view, the optimum temperature of the air reactor is likely in the range of 900 to 925°C for Cu-based oxygen carriers. Research has also been conducted on Cu-based oxygen carriers in the temperature

regime applicable for CLOU in fluidized-bed batch reactors [10, 13, 24-33], continuous operations [27, 34-36] and thermogravimetric studies [28, 37-39], with and without supports.

In cognizance of the potential of copper-based systems as CLOU materials, samples of CuO supported on zirconates of SrZrO<sub>3</sub> and CaZrO<sub>3</sub> were synthesized to assess their suitability as CLOU oxygen carriers. By changing the experimental process variables, such as reaction time and temperature, their tendencies towards the loss of active CuO phase due to the redox operation, agglomeration and particle fragmentation were analyzed.

## 2. Experimental

### 2.1. Preparation and manufacturing of oxygen carriers

The physical properties and characteristics are of the oxygen carriers used in this investigation summarized in Table 1. The samples were prepared via extrusion, described elsewhere in detail [40]. Mixtures consisting of starting component oxides of CuO (Alfa-Aesar, 97 wt.%), SrZrO<sub>3</sub> (Alfa Aesar, 99.3 wt.%) and CaZrO<sub>3</sub> (Thermograde Process Technology), were thoroughly homogenized in a rotary evaporator. After drying, the resulting powder was turned into pliable dough using polyvinyl alcohol (Alfa-Aesar) as dispersant and soluble (C<sub>6</sub>H<sub>10</sub>O<sub>5</sub>)<sub>n</sub> starch (Merck) as binder with additional mixing. LAROSTAT 519 (PPG Industries) which is a quaternary ammonium salt was used as an anti-static agent to increase the flux properties of the mixture. The resulting dough was then processed to form thin strands using a hand-held single screw extruder. The strands were dried in an air oven at 200-220°C overnight and were then calcined in a muffle oven at 950 and 1030°C for a dwelling time of 6 h. The calcined material was sieved through stainless steel screens to yield particles in the range of 125-250 μm.

**Table 1 Physical properties and characteristics of the oxygen carriers used in this work**

Sample	Calcination Temp. [°C]	Active phase, 40 wt. %	Support phase, 60 wt. %	Crushing Strength [N]	Bulk Density [g/cm <sup>3</sup> ]	BET [m <sup>2</sup> /g]
C4SZ-950	950	CuO	SrZrO <sub>3</sub>	0.8	1.46	0.72
C4CZ-950			CaZrO <sub>3</sub>	0.7	1.63	1.98
C4SZ-1030	1030	CuO	SrZrO <sub>3</sub>	1	1.51	1.05
C4CZ-1030			CaZrO <sub>3</sub>	> 0.5	1.25	0.56

### 2.2. Characterization of oxygen carriers

Crystalline phase determination of the oxygen carriers was carried out using powder X-ray diffraction (Bruker AXS, D8 Advanced) with CuK<sub>α1</sub> radiation. The bulk (tapped) density was measured for particles in the size range of 125-180 μm using a graduated cylinder. The Brunauer-Emmett-Teller (BET) specific surface area was measured by N<sub>2</sub>-adsorption (Micromeritics, TriStar 3000). The crushing strength (force needed to fracture a single particle) was measured using a digital force gauge (Shimpo, FGN-5) for particles in the size range of 180-250 μm. An average of 30 measurements was taken as the representative crushing strength. The morphology of the particles was examined with an environmental scanning electron microscope (ESEM) fitted with a field emission gun (FEI, Quanta 200).

### 2.3. Experimental setup and procedure

Experiments for examining oxygen uncoupling and reactivity of the oxygen carriers were carried out in a laboratory-scale quartz fluidized-bed reactor, 870 mm high and 22 mm in inner diameter. The scheme

of the experimental setup used in this investigation is shown in Figure 2. A porous quartz plate was placed at a height of 370 mm from the bottom and the reactor temperature was measured with chromel-alumel (type K) thermocouples sheathed in inconel-600 located about 5 mm below and 25 mm above the plate. Pressure transducers (Honeywell) were used to measure the pressure drop over the bed of particles and the quartz plate at a frequency of 20 Hz. By measuring the fluctuations in the pressure drop, it is possible to determine if the particles were fluidized or not, i.e. a defluidization would be noted from a decrease in pressure fluctuations. The exit gas stream from the reactor was led into a condenser to remove water, which is generated during oxidation of the fuel. The composition of the dry gas was measured by a Rosemount NGA-2000 analyzer, which measured the concentration of O<sub>2</sub> through a paramagnetic channel, CO<sub>2</sub>, CO and CH<sub>4</sub> through infrared channels and H<sub>2</sub> through difference in thermal conductivity of H<sub>2</sub> and N<sub>2</sub>, with correction for other measured gases.

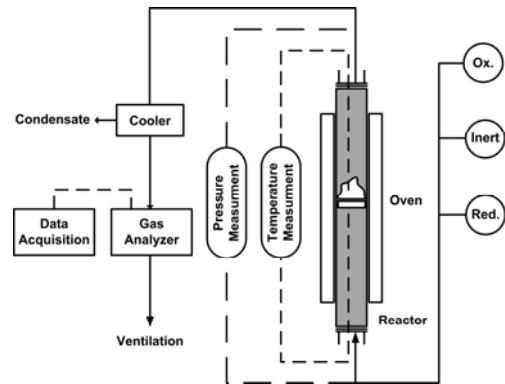


Fig. 2 Scheme of the experimental setup used in this investigation

A sample of 10 g was placed on the porous plate inside the fluidized-bed reactor and the bed was exposed to alternating oxidizing and reducing conditions. Prior to the test, the reactor was heated to 900°C in a stream of 11% O<sub>2</sub> to ensure that the oxygen carrier was in fully oxidized state. In previous investigations using the same experimental setup [13, 40], a 5% O<sub>2</sub> stream was used during the oxidation phase. This was done in order to examine whether the oxygen carrier could be oxidized in an oxygen deficient condition similar to the outlet of the air reactor in a realistic CLC unit. The rationale of using 11% O<sub>2</sub> stream instead in this work was to accelerate the oxidation process. Henceforth, the term cycle will be used to describe a redox cycle involving reduction of the oxygen-carrier sample in inert gas or fuel, followed by oxidation with the aforementioned 11% O<sub>2</sub> mixture. A set of three inert gas cycles were initially carried out for all samples in N<sub>2</sub> to investigate the release of oxygen during a span of 360 s. For reactivity test, methane was primarily used for 10 s during reduction cycles and repeated for at least three times. The duration of 10 s was selected as it approximately corresponds to the reduction of CuO to Cu<sub>2</sub>O in the samples, assuming complete gas conversion. Subsequently, additional cycles were carried out in which the reduction time was increased in steps of 10 s intervals up to 50 s. During the prolonged reduction cycles, it is likely that reduction to Cu is gradually approached, i.e. applicable to CLC. The extended reduction time also helped in evaluating the extent to which the active CuO phase was available for reduction and whether the oxygen carrier could resist agglomeration and particle fragmentation. There was no carbon burn-off during the subsequent oxidation cycles (indicated by way of increase in CO and/or CO<sub>2</sub> concentrations) to show carbon deposition during shorter reduction cycles. This was due to the fact that more oxygen was available than the stoichiometric demand of the fuel. However, some carbon was deposited during the extended reduction cycles as they were depleted of oxygen. Nitrogen was used as an inert purge for 60 s in between oxidation and reduction. Inlet flow rates of 450, 900 and 600 mL<sub>N</sub>/min were used during reduction, oxidation and inert cycle, respectively. These flow rates were chosen to achieve values ranging between 7 to 9  $u_{mf}$  during reduction, 12 to 17  $u_{mf}$  during inert and, 19 to 26  $u_{mf}$  during oxidation of the inlet flows, where  $u_{mf}$  is the minimum fluidization velocity. The minimum fluidization velocity,  $u_{mf}$ , was calculated by using the correlation given by Kunii and Levenspiel [41]. However, it should be noted that due to gas expansion during reduction, the actual velocity in the bed is higher, as CH<sub>4</sub> is converted to CO<sub>2</sub> and H<sub>2</sub>O.

## 2.4. Data analysis

The reactivity of a given oxygen carrier is quantified in terms of gas yield or conversion efficiency,  $\gamma$ , and is defined as the fraction of fully oxidized fuel divided by the carbon containing gases in outlet stream, in this work  $\text{CO}_2$ ,  $\text{CO}$  and  $\text{CH}_4$ .

$$\gamma = \frac{y_{\text{CO}_2}}{y_{\text{CO}_2} + y_{\text{CH}_4} + y_{\text{CO}}} \quad (5)$$

Here  $y_i$  denotes the concentration (vol. %) of the respective gas, obtained from the gas analyzer. The mass-based conversion of the oxygen carrier,  $\omega$ , is defined as

$$\omega = \frac{m}{m_{\text{ox}}} \quad (6)$$

where  $m$  and  $m_{\text{ox}}$  are respectively, the actual mass and the mass of the oxygen carrier in fully oxidized. Equations (7) and (8) are employed for calculating  $\omega$  as a function of time during the reduction and oxidation period respectively from the measured concentrations of various gaseous species by the gas analyzer:

$$\omega_i = \omega_{i-1} - \int_{t_0}^{t_i} \frac{\dot{n}_{\text{out}} M_{\text{O}}}{m_{\text{ox}}} (4y_{\text{CO}_2} + 3y_{\text{CO}} + 2y_{\text{O}_2} - y_{\text{H}_2}) dt \quad (7)$$

$$\omega_i = \omega_{i-1} + \int_{t_0}^{t_i} \frac{2M_{\text{O}}}{m_{\text{ox}}} (\dot{n}_{\text{in}} y_{\text{O}_2, \text{in}} - \dot{n}_{\text{out}} y_{\text{O}_2, \text{out}}) dt \quad (8)$$

where  $\omega_i$  is the instantaneous mass-based conversion at time  $i$ ,  $\omega_{i-1}$  the mass-based conversion in the preceding instant,  $t_0$  and  $t_i$  the initial and final time of measurement,  $M_{\text{O}}$  the molar mass of oxygen, and  $\dot{n}_{\text{out}}$  the molar flow rate of dry gas at the reactor outlet.

## 3. Results

### 3.1. Concentration profiles

Fig. 3 shows the oxygen concentration during the inert gas phase following an oxidation for all samples. During this period,  $\text{CuO}$  decomposes spontaneously into  $\text{Cu}_2\text{O}$  in the environment of inert nitrogen where the particles release oxygen. The oxygen concentrations are somewhat lower than the theoretical equilibrium partial pressure,  $P_{\text{O}_2}$ , corresponding to the decomposition of  $\text{CuO}$  into  $\text{Cu}_2\text{O}$  (1.5% and 2.7% respectively at 900 and 925°C [10]).

Following the inert gas cycles, successful cycles of oxidation and reduction were carried out for all oxygen carriers at 900 and 925°C. As an example, Fig. 4 shows the concentration profile for the C4SZ-1030 sample for the third reduction cycle at 925°C. During the short

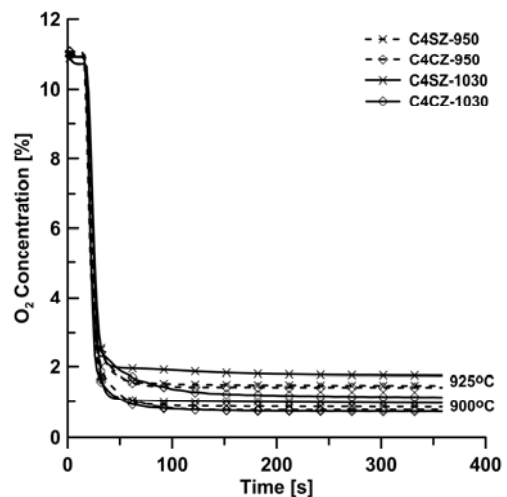


Fig. 3 Oxygen concentrations during inert gas cycles at 900 and 925°C

interval in inert gas prior to fuel injection, the spontaneous release of oxygen via the CLOU mechanism can be seen. The fuel (methane) reacts with the released oxygen, producing CO<sub>2</sub>, with concomitant increase in temperature due to the exothermic nature of the reaction this is common for copper-based oxygen carriers [5]. The rise in temperature shifts the thermodynamic equilibrium and in turn increases the oxygen concentration. However, the actual oxygen concentration during reduction in the reactor is lower due to dilution created by the water formed. This water is removed in the cooler prior to the gas analyzer. Note that no CH<sub>4</sub> or CO was detected during the entire reducing period, and hence full gas yield was clearly achieved. The concentration profiles were similar from cycle to cycle, except for slight variations in peak concentrations due to the transitory non-steady state. At 900°C, less oxygen is released during the inert and reduction cycles.

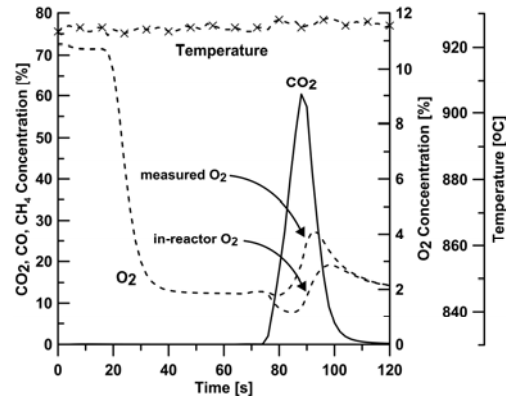


Fig. 4 Concentration and temperature profiles for C4SZ-1030 during reduction for 10 s using CH<sub>4</sub> at 900°C

3.2. Reactivity of oxygen carriers

Fig. 5 shows the reactivity (in terms of gas yield,  $\gamma$ ) for all oxygen carriers at 925°C, using methane as fuel for the third repeated cycle. All samples exhibited high fuel conversion during this period. The carriers lose approximately 2% of their mass as they are converted during 10 s of reduction ( $\omega$  going from 1 to 0.98). Fig. 6 shows the gas yield ( $\gamma$ ) for all samples at 925°C during the extended reduction cycle (50 s) with methane. Under the experimental conditions and the oxygen carriers employed, the theoretical conversion of CuO to Cu,  $\omega$ , at the end of reduction should approach 0.92. This was nearly obtained only in the case of C4CZ-1030 and C4SZ-1030 where  $\omega$  reaches a value of 0.93 with nearly full conversion of methane. On the contrary, in the case of C4CZ-950 and C4SZ-950 samples a lower value of  $\omega$  is reached. This could indicate that the latter two oxygen carriers were not stable during longer reduction periods.

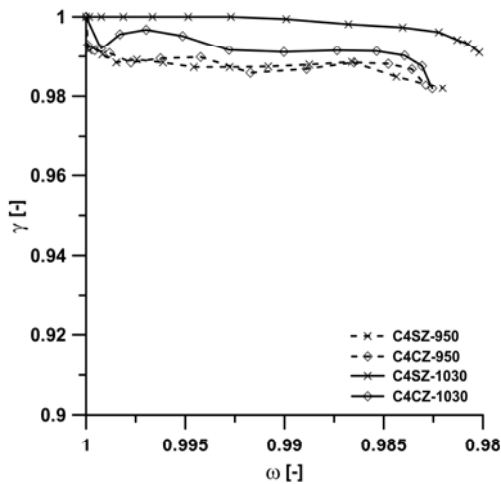


Fig. 5 Gas yield,  $\gamma$ , as a function of mass-based conversion,  $\omega$ , for all oxygen carriers during 10 s of CH<sub>4</sub> reduction at 925°C

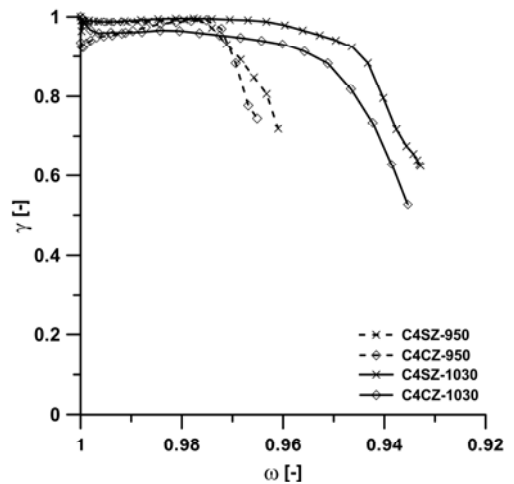


Fig. 6 Gas yield,  $\gamma$ , as a function of mass-based conversion,  $\omega$ , for all oxygen carriers during 50 s of CH<sub>4</sub> reduction at 925°C

Fig. 7 shows the oxygen partial pressure as a function of oxygen carrier conversion,  $\omega$ , in the oxidation phase following the extended reduction period (50 s) at 925°C for the C4CZ-1030 and C4SZ-1030 samples. Note that in Fig. 6, approximately 7% mass-based conversion of the oxygen carriers was reached during 50 s of reduction, i.e.  $\omega$  going from 1 to 0.93. Thus, during the following oxidation cycle, the carrier is expected to retrieve the amount of oxygen withdrawn from the carrier, meaning that  $\omega$  must revert from 0.93 to 1. Only then, truly reversible redox behaviour of the carrier is achieved. For both of the C4CZ-1030 and C4SZ-1030 samples as shown in Fig. 7, the carriers retrieve the expected conversion with the value of  $\omega$  extending to 1. This shows that the active CuO phase has remained intact in these samples.

### 3.3. Physical aspects of the oxygen carriers after redox cycle

The oxygen carrier materials were extracted from the reactor after the experiments for further analysis. The experiments were always ended in the oxidation phase and thus the characterization of the used samples refers to this phase. All samples except the C4SZ-1030 oxygen carrier had experienced sever fragmentation as seen by the large amount of fines formation. Physical characteristics of the fresh oxygen carriers were given in Table 1. The XRD characterization of all fresh and tested samples did not indicate the formation of any ternary compounds other than the active and support phases. The BET surface area of the used C4SZ-1030 sample had decreased to 0.63 m<sup>2</sup>/g.

The ESEM images of fresh and post-reaction for the C4SZ-1030 sample are shown in Fig. 8 (a-b). It can be observed that in this case, the oxygen carrier particles remain individual with no observable agglomeration. However, minor fragmentation could be noticed which requires changes in the preparation and manufacturing method. Considering this and the reactivity test shown in Fig. 5-7, it can be inferred that among investigated oxygen carriers, only C4SZ-1030 could be of interest for the CLOU process.

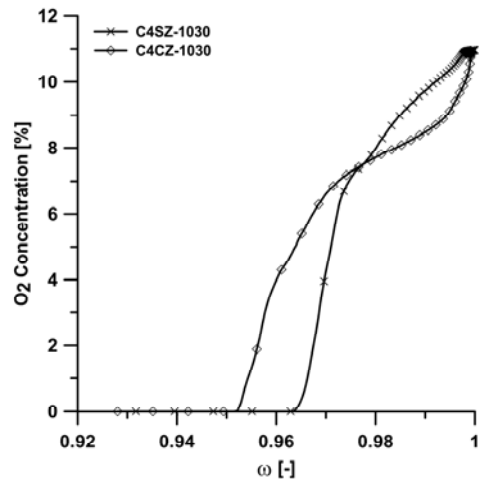


Fig. 7 Variation of oxygen concentration with mass-based conversion ( $\omega$ ) during oxidation at 900°C for C4CZ-1030 and C4SZ-1030

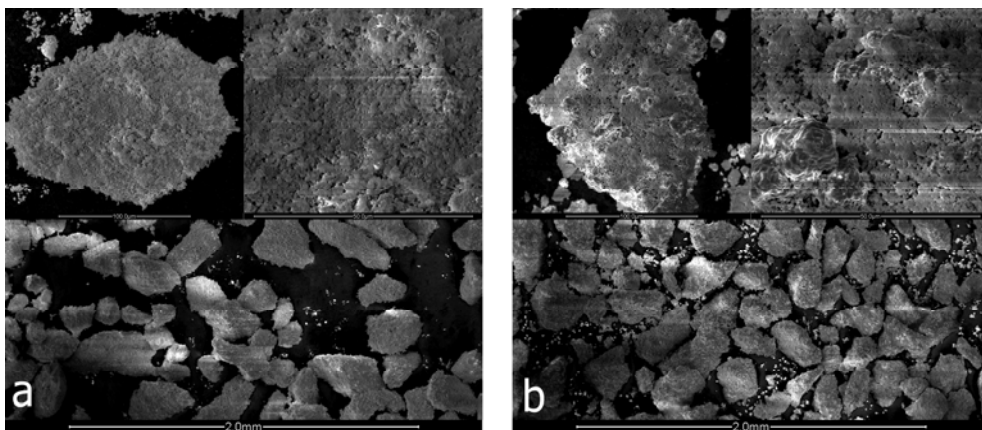


Fig. 8 Fresh (a) and post-reaction (b) ESEM images of C4SZ-1030 oxygen carrier

#### 4. Conclusions

The use of CuO oxygen carriers supported on zirconates of CaZrO<sub>3</sub> and SrZrO<sub>3</sub> as CLOU materials have been investigated. The oxygen carriers were calcined at 950 and 1030°C. All of the investigated oxygen carrier materials showed rapid release of oxygen in an inert environment (CLOU) with high conversion of methane. However, only in the case of SrZrO<sub>3</sub> as support and calcination temperature of 1030°C, deactivation and sever fragmentation were not observed. Thus, the use of this oxygen carrier could be of interest for the CLOU process.

#### Acknowledgements

The authors wish to thank Vattenfall and Chalmers University of Technology via the Energy Area of Advance for the financial support of this work.

#### References

- [1] R.K. Pachauri, A. Reisinger, Fourth Assessment Report: Climate Change (Synthesis Report), Intergovernmental Panel on Climate Change, Geneva, 2007.
- [2] A. Lyngfelt, B. Leckner, T. Mattisson, A fluidized-bed combustion process with inherent CO<sub>2</sub> separation; application of chemical-looping combustion, *Chem. Eng. Sci.* 56 (2001) 3101-3113.
- [3] M. Ishida, H. Jin, A Novel Chemical-Looping Combustor without NO<sub>x</sub> Formation, *Ind. Eng. Chem. Res.* 35 (1996) 2469-2472.
- [4] B. Kronberger, E. Johansson, G. Löffler, T. Mattisson, A. Lyngfelt, H. Hofbauer, A Two-Compartment Fluidized Bed Reactor for CO<sub>2</sub> Capture by Chemical-Looping Combustion, *Chem. Eng. Technol.* 27 (2004) 1318-1326.
- [5] E. Jerndal, T. Mattisson, A. Lyngfelt, Thermal Analysis of Chemical-Looping Combustion, *Chem. Eng. Res. Des.* 84 (2006) 795-806.
- [6] A. Lyngfelt, Oxygen Carriers for Chemical Looping Combustion - 4000 h of Operational Experience, *Oil Gas Sci. Technol.* 66 (2011) 161-172
- [7] A. Lyngfelt, T. Mattisson, Materials for chemical-looping combustion, WILEY-VCH Verlag GmbH & Co. KGaA, Weinheim, 2011.
- [8] M.M. Hossain, H.I. de Lasa, Chemical-looping combustion (CLC) for inherent CO<sub>2</sub> separations-a review, *Chem. Eng. Sci.* 63 (2008) 4433-4451.
- [9] J. Adanez, A. Abad, F. Garcia-Labiano, P. Gayan, L.F. de Diego, Progress in Chemical-Looping Combustion and Reforming technologies, *Progr. Energy Combust. Sci.* 38 (2012) 215-282.
- [10] T. Mattisson, A. Lyngfelt, H. Leion, Chemical-looping with oxygen uncoupling for combustion of solid fuels, *Int. J. Greenhouse Gas Control* 3 (2009) 11-19.
- [11] S.Y. Chuang, J.S. Dennis, A.N. Hayhurst, S.A. Scott, Development and performance of Cu-based oxygen carriers for chemical-looping combustion, *Combust. Flame* 154 (2008) 109-121.
- [12] J.S. Dennis, C.R. Müller, S.A. Scott, In situ gasification and CO<sub>2</sub> separation using chemical looping with a Cu-based oxygen carrier: Performance with bituminous coals, *Fuel* 89 (2010) 2353-2364.
- [13] M. Arjmand, A.-M. Azad, H. Leion, A. Lyngfelt, T. Mattisson, Prospects of Al<sub>2</sub>O<sub>3</sub> and MgAl<sub>2</sub>O<sub>4</sub>-Supported CuO Oxygen Carriers in Chemical-Looping Combustion (CLC) and Chemical-Looping with Oxygen Uncoupling (CLOU), *Energy Fuels* 25 (2011) 5493-5502.
- [14] C.R. Forero, P. Gayán, F. García-Labiano, L.F. de Diego, A. Abad, J. Adánez, High temperature behaviour of a CuO/γAl<sub>2</sub>O<sub>3</sub> oxygen carrier for chemical-looping combustion, *Int. J. Greenhouse Gas Control* 5 (2011) 659-667.
- [15] P. Gayán, C.R. Forero, A. Abad, L.F. de Diego, F. García-Labiano, J. Adánez, Effect of Support on the Behavior of Cu-Based Oxygen Carriers during Long-Term CLC Operation at Temperatures above 1073 K, *Energy Fuels* 25 (2011) 1316-1326.
- [16] T. Mattisson, A. Järndäs, A. Lyngfelt, Reactivity of Some Metal Oxides Supported on Alumina with Alternating Methane and Oxygen Application for Chemical-Looping Combustion, *Energy Fuels* 17 (2003) 643-651.
- [17] L.F. de Diego, P. Gayán, F. García-Labiano, J. Celaya, A. Abad, J. Adánez, Impregnated CuO/Al<sub>2</sub>O<sub>3</sub> Oxygen Carriers for Chemical-Looping Combustion: Avoiding Fluidized Bed Agglomeration, *Energy Fuels* 19 (2005) 1850-1856.
- [18] L.F. de Diego, F. García-Labiano, P. Gayán, J. Celaya, J.M. Palacios, J. Adánez, Operation of a 10 kWth chemical-looping combustor during 200 h with a CuO-Al<sub>2</sub>O<sub>3</sub> oxygen carrier, *Fuel* 86 (2007) 1036-1045.
- [19] M. Arjmand, A.-M. Azad, H. Leion, T. Mattisson, A. Lyngfelt, Evaluation of CuAl<sub>2</sub>O<sub>4</sub> as an Oxygen Carrier in Chemical-Looping Combustion, *Ind. Eng. Chem. Res.* 51 (2012) 13924-13934.
- [20] B. Wang, H. Zhao, Y. Zheng, Z. Liu, R. Yan, C. Zheng, Chemical looping combustion of a Chinese anthracite with Fe<sub>2</sub>O<sub>3</sub>-based and CuO-based oxygen carriers, *Fuel Process. Technol.* 96 (2012) 104-115.

- [21] L.F. de Diego, F. García-Labiano, J. Adánez, P. Gayán, A. Abad, B.M. Corbella, J. María Palacios, Development of Cu-based oxygen carriers for chemical-looping combustion, *Fuel* 83 (2004) 1749-1757.
- [22] S.Y. Chuang, J.S. Dennis, A.N. Hayhurst, S.A. Scott, Kinetics of the chemical looping oxidation of H<sub>2</sub> by a co-precipitated mixture of CuO and Al<sub>2</sub>O<sub>3</sub>, *Chem. Eng. Res. Des.* 89 (2011) 1511-1523.
- [23] K.W. Lewis, E.R. Gilliland, M.P. Sweeney, Gasification of Carbon Metal Oxides in a Fluidized Powder Bed, *Chem. Eng. Prog.* 47 (1951) 251-256.
- [24] T. Mattisson, H. Leion, A. Lyngfelt, Chemical-looping with oxygen uncoupling using CuO/ZrO<sub>2</sub> with petroleum coke, *Fuel* 88 (2009) 683-690.
- [25] M. Arjmand, M. Keller, H. Leion, T. Mattisson, A. Lyngfelt, Oxygen Release and Oxidation Rates of MgAl<sub>2</sub>O<sub>4</sub>-Supported CuO Oxygen Carrier for Chemical-Looping Combustion with Oxygen Uncoupling (CLOU), *Energy Fuels* 26 (2012) 6528-6539.
- [26] I. Adánez-Rubio, A. Abad, P. Gayán, L.F. de Diego, F. García-Labiano, J. Adánez, Identification of operational regions in the Chemical-Looping with Oxygen Uncoupling (CLOU) process with a Cu-based oxygen carrier, *Fuel* 102 (2012) 635-645.
- [27] I. Adánez-Rubio, P. Gayán, A. Abad, L.F. de Diego, F. García-Labiano, J. Adánez, Evaluation of a Spray-Dried CuO/MgAl<sub>2</sub>O<sub>4</sub> Oxygen Carrier for the Chemical Looping with Oxygen Uncoupling Process, *Energy Fuels* 26 (2012) 3069-3081.
- [28] P. Gayán, I. Adánez-Rubio, A. Abad, L.F. de Diego, F. García-Labiano, J. Adánez, Development of Cu-based oxygen carriers for Chemical-Looping with Oxygen Uncoupling (CLOU) process, *Fuel* 96 (2012) 226-238.
- [29] M. Arjmand, H. Leion, M. Mattisson, A. Lyngfelt, ZrO<sub>2</sub>-Supported CuO Oxygen Carriers for Chemical-Looping with Oxygen Uncoupling (CLOU), *Energy Procedia* (2013).
- [30] M. Arjmand, A.-M. Azad, H. Leion, M. Rydén, M. Mattisson, CaZrO<sub>3</sub> and SrZrO<sub>3</sub>-supported CuO Oxygen Carriers for Chemical-looping with Oxygen Uncoupling (CLOU), *Energy Procedia* (2013).
- [31] H. Leion, T. Mattisson, A. Lyngfelt, Using chemical-looping with oxygen uncoupling (CLOU) for combustion of six different solid fuels, *Energy Procedia* 1 (2009) 447-453.
- [32] A. Hedayati, A.-M. Azad, M. Rydén, H. Leion, T. Mattisson, Evaluation of Novel Ceria-Supported Metal Oxides As Oxygen Carriers for Chemical-Looping Combustion, *Ind. Eng. Chem. Res.* 51 (2012) 12796-12806.
- [33] I. Adánez-Rubio, M. Arjmand, H. Leion, P. Gayán, A. Abad, T. Mattisson, A. Lyngfelt, Investigation of Combined Supports for Cu-Based Oxygen Carriers for Chemical-Looping with Oxygen Uncoupling (CLOU), *Energy Fuels* 27 (2013) 3918-3927.
- [34] A. Abad, I. Adánez-Rubio, P. Gayán, F. García-Labiano, L.F. de Diego, J. Adánez, Demonstration of chemical-looping with oxygen uncoupling (CLOU) process in a 1.5 kW<sub>th</sub> continuously operating unit using a Cu-based oxygen-carrier, *Int. J. Greenhouse Gas Control* 6 (2012) 189-200.
- [35] I. Adánez-Rubio, A. Abad, P. Gayán, L.F. de Diego, F. García-Labiano, J. Adánez, Performance of CLOU process in the combustion of different types of coal with CO<sub>2</sub> capture, *Int. J. Greenhouse Gas Control* 12 (2013) 430-440.
- [36] P. Moldenhauer, M. Rydén, T. Mattisson, A. Lyngfelt, Chemical-looping combustion and chemical-looping with oxygen uncoupling of kerosene with Mn- and Cu-based oxygen carriers in a circulating fluidized-bed 300W laboratory reactor, *Fuel Process. Technol.* 104 (2012) 378-389.
- [37] L. Xu, J. Wang, Z. Li, N. Cai, Experimental Study of Cement-Supported CuO Oxygen Carriers in Chemical Looping with Oxygen Uncoupling (CLOU), *Energy Fuels* 27 (2013) 1522-1530.
- [38] E.M. Eyring, G. Konya, J.S. Lighty, A.H. Sahir, A.F. Sarofim, K. Whitty, Chemical Looping with Copper Oxide as Carrier and Coal as Fuel, *Oil Gas Sci. Technol.* 66 (2011) 209-221.
- [39] Y.-y. Wen, Z.-s. Li, L. Xu, N.-s. Cai, Experimental Study of Natural Cu Ore Particles as Oxygen Carriers in Chemical Looping with Oxygen Uncoupling (CLOU), *Energy Fuels* 26 (2012) 3919-3927.
- [40] M. Arjmand, A. Hedayati, A.-M. Azad, H. Leion, M. Rydén, T. Mattisson, Ca<sub>x</sub>La<sub>1-x</sub>Mn<sub>1-y</sub>M<sub>y</sub>O<sub>3-δ</sub> (M = Mg, Ti, Fe, or Cu) as Oxygen Carriers for Chemical-Looping with Oxygen Uncoupling (CLOU), *Energy Fuels* 27 (2013) 4097-4107.
- [41] D. Kunii, O. Levenspiel, *Fluidization Engineering*, Butterworth-Heinemann, Boston, 1991.